PHILOSOPHICAL TRANSACTIONS A

rsta.royalsocietypublishing.org

Research

Cite this article: Bacon S, Aksenov Y, Fawcett S, Madec G. 2015 Arctic mass, freshwater and heat fluxes: methods and modelled seasonal variability. *Phil. Trans. R. Soc. A* **373**: 20140169. http://dx.doi.org/10.1098/rsta.2014.0169

Accepted: 13 July 2015

One contribution of 6 to a discussion meeting issue 'Arctic sea ice reduction: the evidence, models and impacts (Part 2)'.

Subject Areas:
oceanography, glaciology, climatology

Keywords:
Arctic, fluxes, mass, freshwater, heat

Author for correspondence:
Sheldon Bacon
e-mail: s.bacon@noc.ac.uk

Arctic mass, freshwater and heat fluxes: methods and modelled seasonal variability

Sheldon Bacon[1], Yevgeny Aksenov[1], Stephen Fawcett[1] and Gurvan Madec[1,2]

[1]National Oceanography Centre, Southampton SO14 3ZH, UK
[2]Laboratoire d'Océanographie et du Climat, Université Pierre et Marie Curie, Paris, France

Considering the Arctic Ocean (including sea ice) as a defined volume, we develop equations describing the time-varying fluxes of mass, heat and freshwater (FW) into, and storage of those quantities within, that volume. The seasonal cycles of fluxes and storage of mass, heat and FW are quantified and illustrated using output from a numerical model. The meanings of 'reference values' and FW fluxes are discussed, and the potential for error through the use of arbitrary reference values is examined.

1. Introduction

The Arctic is changing rapidly [1], the signal of surface-based 'Arctic amplification' has emerged from the background [2], the potential of Arctic-sourced freshwater (FW) to perturb Atlantic Ocean northwards heat fluxes is well recognized (e.g. [3]), and recent work has identified mechanisms whereby Arctic warming may impact mid-latitude, regional weather [4–7]. Yet our knowledge of the Arctic itself remains poor, and this is well illustrated by Cowtan & Way [8], who develop methods for reconstructing surface temperatures in poorly sampled regions of the planet, including the Arctic. They note that present evidence from all sources, whether extrapolations, reanalysis products, or satellite lower troposphere measurements, indicates strongly increasing trends in Arctic surface temperatures, while surface measurements in the region remain very sparse, particularly over the ocean and sea ice.

In this context, we have been exploring the utility of an important source of *in situ* measurements, in the form of an array of sustained, fixed ocean installations (moored current meters with temperature and salinity sensors).

THE ROYAL SOCIETY PUBLISHING

These installations describe a closed circuit around the Arctic boundary, where the boundary comprises either measurements in a set of Arctic Ocean gateways, or land. The approach and measurement locations are described in Tsubouchi *et al.* [9], wherein quasi-synoptic boundary measurements are used to calculate surface fluxes of heat and FW. The approach has been extended to the calculation of Arctic ocean inorganic nutrient and carbon fluxes [10,11] and is presently being further extended to analyse a full annual cycle of surface heat and FW fluxes.

The well-defined boundary locations enable the transfer of the approach to the modelling realm where the analogous quantities may be calculated, with the eventual aim of using measurement-derived products to validate their modelled equivalents. This study has two motivations: first, to develop further the boundary flux calculation method; and second, to explore the application of the method as it applies to ocean storage of mass, heat and FW—quantities which are hard to estimate directly from measurements. As an ancillary aim, we are interested to clarify the role assumed by 'reference values', which commonly appear in ocean flux calculations, and are seldom well defined.

In this paper, therefore, we will firstly describe the model architecture and range of configurations and surface forcing data available to us (§2), then derive the equations for calculation of surface fluxes and storage from boundary data (§3). In §4, we illustrate and discuss the outputs resulting from the approach developed in §3. Section 5 contains a discussion of 'reference values' and FW fluxes, and the errors consequent on use of arbitrary reference values are examined.

2. Model

The Nucleus for European Modelling of the Ocean (NEMO) is a widely used framework for oceanographic modelling. It performs well in the Arctic: e.g. Jahn *et al.* [12], Lique & Steele [13], Bacon *et al.* [14]. NEMO uses the primitive equation model Ocean Parallelisé (OPA 9.1) [15] coupled with the Louvain-la-Neuve sea ice model (LIM2) [16]. The model is discretized on a tripolar grid with two northern poles (one in Siberia, one in Canada) and the geographical South Pole. A detailed bathymetry is used by modification of the 2 min gridded global relief Earth Topography (ETOPO2v2), which contains Smith & Sandwell [17] satellite data between 72° N and 72° S, the International Bathymetric Chart of the Arctic Ocean (IBCAO) [18] above 72° N, and the 5 min gridded Digital Bathymetric Data Base (DBDB5) south of 72° S. Description of ETOPO2v2 is available from the National Geophysical Data Center of the US National Oceanic and Atmospheric Administration via their website at http://www.ngdc.noaa.gov/, and description of DBDB5 by the US Naval Oceanographic Office via the Global Master Change Directory of the US National Aeronautics and Space Administration website at http://gcmd.nasa.gov/.

The ocean component of NEMO solves the Navier–Stokes equations using the Boussinesq approximation, in which density is considered constant and is called the reference density (ρ_0), except when solving the hydrostatic balance equation. In the Boussinesq approximation, mass conservation reduces to the incompressibility equation, so that the model conserves volume (considered also as Boussinesq mass, which is a product of volume and ρ_0) rather than mass. The horizontal momentum balance is also approximated with constant ρ_0. The hydrostatic balance, described by Madec *et al.* [15], uses *in situ* density in a formulation originally due to Jackett & McDougall [19].

Initial values of sea temperature and salinity are obtained from the World Ocean Atlas (WOA) [20,21] merged with the Polar Hydrographic Climatology (PHC) v. 2.1 database [22] in high latitudes. The sea surface salinity is relaxed toward the monthly mean from WOA, which has a resolution of 1° latitude by 1° longitude. The relaxation is equivalent to restoring model salinity observed in the top 50 m on a time scale of 180 days.

Two model configurations are used in the present analysis, ORCA0083 with 1/12° mean horizontal resolution and ORCA025 with 1/4° mean horizontal resolution. NEMO's tripolar grid amplifies resolution in the Arctic to approximately 3 km (ORCA0083) and approximately 9 km (ORCA025). The Arctic Ocean Rossby radius is of order 10 km in the deep basins but can be

less than 1 km over the shallow shelf seas [23], so ORCA0083 is eddy-resolving in the deep basins but eddy-permitting at best over the shelves, while ORCA025 is only eddy-permitting in the deep basins. Since ORCA0083 is eddy-resolving in most of the world ocean, there is no parametrization for lateral mixing due to eddies. In the vertical, both versions contain 75 levels from the surface to 5900 m, and layers increase in thickness from 1 m at the surface to 204 m at the bottom; 29 levels cover the first 150 m. In addition, partial steps in the model bottom topography are used to improve model approximation of the steep seabed relief near the continental shelves [24]. The ocean free surface is linear in ORCA025 and nonlinear in ORCA0083 [25]. An iso-neutral Laplacian operator is used for lateral tracer diffusion. A bi-Laplacian horizontal operator is applied for momentum diffusion. A turbulent kinetic energy (TKE) closure scheme is used for vertical mixing. It incorporates background TKE values for vertical eddy viscosity of $10^{-4}\,\mathrm{m^2\,s^{-1}}$ and for vertical eddy diffusivity of $10^{-5}\,\mathrm{m^2\,s^{-1}}$ [15].

Model atmospheric forcing for ORCA0083 is the DRAKKAR Forcing Set (DFS4) reanalysis and is described by Brodeau *et al*. [26]. Atmospheric features of this dataset are drawn from the Common Ocean Reference Experiment, phase II (CORE-II) [27] and the European Centre for Medium-range Weather Forecasts (ECMWF) [28]. Air–sea and air–ice fluxes are calculated by atmospheric boundary layer formulations [29]. For ORCA025, CORE-II and ERA-Interim atmospheric forcings are used [26,29].

In this study, four model runs are used, three of which employ the ORCA025 configuration and one ORCA0083. The ORCA0083 run is forced with DFS4 and integrated for 1978–2010, with output from 1981 analysed here. The ORCA025 runs are: (i) run 1958–2007 forced with CORE-II ('long') and output from 1981 analysed here, (ii) run 1989–2007 forced with CORE-II ('short'), and (iii) 1989–2011 forced with ERA-Interim. The full record of the latter two runs is analysed here. The 'long' and 'short' CORE-II-forced runs differ in start date only. For the transport and surface flux calculations, monthly mean fields are used, while to obtain rate changes in volume, salinity and temperature the instantaneous fields are used. The model timestep is 1440 s for ORCA025 integrations and 200 s for ORCA0083. Seasonal cycles are generated as 12 mean calendar months for each run.

Actual measurement locations are shown in Tsubouchi *et al*. [9]. We slightly simplify the definition of the boundary, in order that it conform to meridians of longitude and parallels of latitude. The Arctic Ocean is enclosed by sections across the four main gateways—Fram, Davis and Bering Straits, and the Barents Sea Opening (BSO), enclosing an ice–ocean surface area of $1.4 \times 10^{13}\,\mathrm{m^2}$. The gateway locations are defined as:

Fram Strait: coast-to-coast, Greenland to Svalbard, across 79° N
Davis Strait: coast-to-coast, Baffin Island to Greenland, across 67° N
Bering Strait: coast-to-coast, Siberia to Alaska, across 65.75° N
BSO: coast-to-coast, Norway to Svalbard, up 19° E.

Finally, we note that Fury and Hecla Strait, between the Melville Peninsula on the Canadian mainland and the northwest of Baffin Island, is extremely narrow at its eastern end. Two islands separate the strait into three channels; the largest is approximately 2 km wide, the others a couple of hundred metres wide. As discussed in Tsubouchi *et al*. [9], the evidence for a significant net through-flow out of the Arctic via Fury and Hecla Strait and (eventually) into the Labrador Sea is ambiguous. Nevertheless, if the strait is open in a model (as it is in ORCA0083), it should be included as part of the boundary.

3. Material and methods

(a) Basics

We define a closed volume V bounded by area A, on the surface of which the normal direction is described by the unit vector $\boldsymbol{n}$. The direction of $\boldsymbol{n}$ is defined as positive-inwards—opposite to the

usual definition—so that when applied to the Arctic Ocean, polewards ice and ocean velocities are positive. For a vector flux $\boldsymbol{F}$, Gauss's theorem then states

$$\iiint (\nabla \cdot \boldsymbol{F})\, \mathrm{d}V = -\iint \boldsymbol{F} \cdot \boldsymbol{n}\, \mathrm{d}A. \tag{3.1}$$

Fluxes of mass (m) or a scalar quantity (Q) are given by

$$\boldsymbol{F}_m = \rho \boldsymbol{u} \tag{3.2}$$

and

$$\boldsymbol{F}_Q = \rho Q \boldsymbol{u} - \rho \kappa_Q \nabla Q, \tag{3.3}$$

where $\boldsymbol{u}$ is vector velocity, ρ is density and κ_Q is a diffusivity, and conservation equations for m and Q take the forms [30]

$$\nabla \cdot (\rho \boldsymbol{u}) = -\frac{\partial \rho}{\partial t} \tag{3.4}$$

and

$$\nabla \cdot (\rho Q \boldsymbol{u} - \rho \kappa_Q \nabla Q) = -\frac{\partial (\rho Q)}{\partial t}. \tag{3.5}$$

In the marine context, the closed volume is defined as follows. Its continuous side-wall boundary comprises either sea ice and ocean at fixed geographical positions (defined by the latitude and longitude of measurement locations) or coastline. Its bottom boundary is the sea bed, which is taken to be impermeable. Its upper boundary is defined as the ocean surface (in the absence of sea ice), or as the upper surface of the sea ice (in its presence). Seawater and sea ice comprise an integral system which exchanges mass between solid and liquid components through the freeze–melt cycle. The upper boundary is mobile, so that the sea surface height is a time-varying function of latitude and longitude. Equations (3.3) and (3.5) are simplified by noting that ocean and sea ice measurements are made in a vertical plane, so that ∇ is replaced by ∇_{H}, where H indicates horizontal components. Furthermore, measured section locations are chosen to be cross-stream, so that $\kappa_Q \nabla_{\mathrm{H}} Q \ll Qu$, where u is horizontal (scalar) speed normal to the section. As an illustration applied to salinity, we take typical ocean values of salinity approximately 35, $u \sim 0.1\,\mathrm{m\,s^{-1}}$, their product being 3.5. With horizontal diffusivity $\kappa \sim 1000\,\mathrm{m^2\,s^{-1}}$, and an along-stream salinity gradient due to mixing of order 1 in salinity over 1000 km (i.e. $10^{-6}\,\mathrm{m^{-1}}$), their product is approximately 10^{-3}. Along-stream horizontal diffusive transports of scalars are therefore a few orders of magnitude smaller than horizontal advective transports, so that (3.3) and (3.5) become, to a good approximation,

$$\boldsymbol{F}_Q = \rho Q \boldsymbol{u} \tag{3.6}$$

and

$$\nabla \cdot (\rho Q \boldsymbol{u}) = -\frac{\partial (\rho Q)}{\partial t}. \tag{3.7}$$

We are interested in practical time scales on which seasonal variability of fluxes and storage may be calculated, and on which short-term 'noise', such as transient responses to weather, may be excluded by averaging, so we consider two wave propagation time scales. External Kelvin and gravity waves are fast, with phase speeds (c_{g}) given by

$$c_{\mathrm{g}} = \sqrt{gH}, \tag{3.8}$$

where H is now water depth, set to a scale value of 1000 m and g (acceleration due to gravity) is $10\,\mathrm{m\,s^{-2}}$, giving $c = 100\,\mathrm{m\,s^{-1}}$, which will cover a scale distance of 1000 km in a few hours. The phase speed of a long barotropic Rossby wave (c_{R}) is

$$c_{\mathrm{R}} = \frac{\beta g H}{f^2}, \tag{3.9}$$

where f is the Coriolis parameter and β its meridional gradient. Using values of f and β appropriate to 80° N, we find $c_R \sim 2\,\mathrm{m\,s^{-1}}$, and the time to cover 1000 km is then approximately one week. As a result, we consider one month to be a sensible (conservative and conventional) time scale on which to base subsequent calculations.

(b) Mass and freshwater fluxes

We first consider Gauss's theorem as applied to the mass flux (3.2), by decomposing the integral on the RHS of (3.1):

$$\iint (\rho \boldsymbol{u}) \cdot \boldsymbol{n} \, \mathrm{d}A = \iint \rho v \, \mathrm{d}s \, \mathrm{d}z + F_{\mathrm{m}}^{\mathrm{surf}}. \tag{3.10}$$

There is no normal flow at the seabed, v is the inwards-positive component of ice or ocean velocity normal to the ice and ocean side boundary, and s and z are horizontal (along-boundary) and vertical coordinates, respectively. $F_{\mathrm{m}}^{\mathrm{surf}}$ is the (net) surface mass flux entering the ocean, which in reality is the sum of three terms: precipitation into and evaporation from the ocean, and run-off from land into the ocean. We next take the LHS of (3.1) and substitute (3.4), still considering mass flux:

$$\iiint (\nabla \cdot \rho \boldsymbol{u}) \, \mathrm{d}V = - \iiint \left(\frac{\partial \rho}{\partial t} \right) \mathrm{d}V = -\dot{M}, \tag{3.11}$$

where M is total mass within the defined volume and $\dot{M} = \partial M / \partial t$ is the rate of change of mass within the volume: i.e. mass storage. The final step reverses the order of operations, noting that $\iiint \rho \, \mathrm{d}V = M$. Combining (3.1), (3.10) and (3.11), and writing $F_{\mathrm{m}}^{\mathrm{io}} = \iint \rho v \, \mathrm{d}s \, \mathrm{d}z$ as the side-boundary ice and ocean mass flux, we obtain

$$F_{\mathrm{m}}^{\mathrm{surf}} + F_{\mathrm{m}}^{\mathrm{io}} = \dot{M}. \tag{3.12}$$

In the stationary case where $\dot{M} = 0$, any surface mass input ($F_{\mathrm{m}}^{\mathrm{surf}}$ positive) is exactly balanced by ice and ocean side-boundary outflow ($F_{\mathrm{m}}^{\mathrm{io}}$ negative) from the volume. Considering the mass storage term, imagine a simple case where the side boundaries are all closed and the surface mass flux is positive; therefore, the sea level will rise. In terms of the defined volume and mobile upper surface, this represents a gain of mass by the volume.

We now consider Gauss's theorem as applied to the salinity (S) flux, replacing Q in (3.6), by decomposing the integral on the RHS of (3.1):

$$\iint (S \rho \boldsymbol{u}) \cdot \boldsymbol{n} \, \mathrm{d}A = \iint S \rho v \, \mathrm{d}s \, \mathrm{d}z. \tag{3.13}$$

This is analogous to (3.10), but with no surface pathway for salinity. Taking the LHS of (3.1) and substituting (3.7) for salinity, we obtain

$$\iiint (\nabla \cdot S \rho \boldsymbol{u}) \, \mathrm{d}V = - \iiint \left(\frac{\partial S \rho}{\partial t} \right) \mathrm{d}V = -\dot{M}_{\mathrm{s}}, \tag{3.14}$$

where $\iiint \rho S \, \mathrm{d}V = M_{\mathrm{S}}$ is the mass of salt within the defined volume and $\dot{M} = \partial M_{\mathrm{s}} / \partial t$. Combining (3.1), (3.13) and (3.14) gives

$$\iint S \rho v \, \mathrm{d}s \, \mathrm{d}z = \dot{M}_{\mathrm{s}}, \tag{3.15}$$

so that any imbalance between inflow and outflow of salinity results in a change in stored salinity. To proceed, we next define means and anomalies from means, for S (3.16) and for the product ρv (3.17). The averaging operator is the area-mean, and it is important that, by construction, the mean of the anomaly is identically zero.

$$S = \bar{S} + S', \tag{3.16a}$$

$$\bar{S} = \frac{\iint S \, \mathrm{d}s \, \mathrm{d}z}{\iint \mathrm{d}s \, \mathrm{d}z}, \tag{3.16b}$$

$$\iint S' \, \mathrm{d}s \, \mathrm{d}z = 0, \tag{3.16c}$$

$$\rho v = \overline{(\rho v)} + (\rho v)', \tag{3.17a}$$

$$\overline{(\rho v)} = \frac{\iint (\rho v)\,\mathrm{d}s\,\mathrm{d}z}{\iint \mathrm{d}s\,\mathrm{d}z} \tag{3.17b}$$

and

$$\iint (\rho v)'\,\mathrm{d}s\,\mathrm{d}z = 0. \tag{3.17c}$$

Expanding the LHS of (3.15) using (3.16) and (3.17) gives

$$\iint S\rho v\,\mathrm{d}s\,\mathrm{d}z = \iint [\overline{(\rho v)} + (\rho v)'][\bar{S} + S']\,\mathrm{d}s\,\mathrm{d}z = \iint \overline{(\rho v)} \cdot \bar{S}\,\mathrm{d}s\,\mathrm{d}z + \iint (\rho v)' S'\,\mathrm{d}s\,\mathrm{d}z. \tag{3.18}$$

The cross-terms in the expansion of (3.18) are the integrals of the products of means with anomalies: $[\bar{S}(\rho v)']$ and $[\overline{(\rho v)}S']$. Their integrals equal zero by construction of the anomalies. The two terms on the RHS of (3.18) remain, the second of which is the integral of the product of the anomalies. The first term on the RHS of (3.18) is simply the product of $\bar{S}$ with $F_{\mathrm{m}}^{\mathrm{io}}$, so that (3.15) becomes

$$\iint (\rho v)' S'\,\mathrm{d}s\,\mathrm{d}z + \bar{S}F_{\mathrm{m}}^{\mathrm{io}} = \dot{M}_{\mathrm{s}}. \tag{3.19}$$

Next we multiply (3.12) by $\bar{S}$ to obtain

$$\bar{S}F_{\mathrm{m}}^{\mathrm{surf}} + \bar{S}F_{\mathrm{m}}^{\mathrm{io}} = \bar{S}\dot{M}. \tag{3.20}$$

We eliminate common terms between (3.19) and (3.20) and rearrange, to obtain

$$F_{\mathrm{m}}^{\mathrm{surf}} = \frac{\iint (\rho v)' S'\,\mathrm{d}s\,\mathrm{d}z}{\bar{S}} + \dot{M} - \frac{\dot{M}_{\mathrm{s}}}{\bar{S}}. \tag{3.21}$$

The Boussinesq approximation explicitly assumes constant density, so that (3.21) becomes an expression in volume (subscript 'vol') fluxes:

$$F_{\mathrm{vol}}^{\mathrm{surf}} = \frac{\iint v' S'\,\mathrm{d}s\,\mathrm{d}z}{\bar{S}} + \dot{V} - \frac{1}{\bar{S}}\left[\frac{\partial}{\partial t}\iiint S\,\mathrm{d}V\right]. \tag{3.22}$$

For completeness, (3.12) is similarly re-cast:

$$F_{\mathrm{vol}}^{\mathrm{surf}} + F_{\mathrm{vol}}^{\mathrm{io}} = \dot{V}. \tag{3.23}$$

In NEMO, volume changes result from movement of the free surface. The volume forms are also suitable for transport and storage calculations based on hydrographic measurements, which typically employ volume rather than mass fluxes.

Consider the terms in (3.21) and (3.22). The first term on the RHS is the ice and ocean FW boundary flux. In the stationary case, the time-varying terms equal zero, so that the boundary flux is equal to the surface flux. In a (simplified) version of the Arctic Ocean case, saline waters enter the Arctic and fresher waters leave. The dilution is performed by the surface flux, and ice and ocean boundary measurements of velocity and salinity can, therefore, be used to calculate the surface flux: for example, for a positive surface flux (FW input), a saline (S' positive) inflow (v' positive) will be diluted into a fresh (S' negative) outflow (v' negative)—all contributing components are positive. This calculation was applied to Arctic boundary measurements made in September 2005 by Tsubouchi *et al*. [9].

The second term on the RHS of (3.21) and (3.22) is the rate of change of mass (or volume) within the defined volume, and we call this the storage flux. A surface input may be retained within the boundary—e.g. by mechanical forcing such as Ekman pumping—and it contributes to the calculation of the total surface flux. The third term is the rate of change of the quantity of salt within the defined volume (scaled by boundary-mean salinity), and we call this the 'dilution flux'. If the salinity within the defined volume increases, this then represents a loss of FW from the defined volume. These, then, are complete (i.e. including time-variation) equations for calculating surface FW flux, either as mass or volume fluxes. Ideally, in the real world, the LHS of (3.21) and (3.22) would be directly measured. However, this is difficult, so the RHS of (3.21) and (3.22)

shows what must be measured in the ocean and sea ice system in order to calculate the surface FW flux indirectly.

(c) Heat fluxes

Several authors have considered the calculation of what is called 'heat flux' in the context of the fluid (atmosphere and ocean) environment, including Starr [31], Bryan [32], Gill [30], Saunders [33], Bacon & Fofonoff [34], Warren [35] and McDougall [36]. The general problem concerns the finding of a correct expression of the first law of thermodynamics, which has led these authors to consider fluxes of internal energy [31,35], the total energy via the Bernoulli function [33], and the enthalpy, including the definition of two new quantities, potential enthalpy and conservative temperature [36]. These papers all find ways to eliminate mechanical (large-scale kinetic and potential) energy as a consideration, but are all left with the mechanical dissipation of kinetic energy as heat at the molecular level, which must be ignored as negligible. Therefore, we pursue an approach combining those of McDougall [36] (his eqn (28)) and Serreze *et al*. [37] (their eqns (4) and (5)), while considering uncertainties arising from various approximations.

The heat budget of the water column from the surface (including sea ice) to the sea bed is

$$\frac{\partial(\Sigma\rho H^{\mathrm{io}})}{\partial t} + \nabla\cdot(\Sigma\rho \boldsymbol{u} H^{\mathrm{io}}) = -\nabla\cdot \boldsymbol{F}_{\mathrm{H}}^{\mathrm{bdy}} + \rho\epsilon, \tag{3.24}$$

where H^{io} is the heat stored per unit mass ($\mathrm{J\,kg^{-1}}$) in the ice–ocean system, which comprises the latent heat stored in ice, and the sensible heat stored in ice and ocean. In the first term on the LHS, $\Sigma\rho H^{\mathrm{io}}$ represents the sum of these components multiplied by the relevant density (for solid or liquid phases) to produce the total heat stored per unit volume ($\mathrm{J\,m^{-3}}$). This quantity expands, with superscript o for liquid ocean and superscript i for sea ice, as

$$\Sigma\rho H^{\mathrm{io}} = (\rho c_{\mathrm{p}}\theta)^{\mathrm{o}} + (\rho c_{\mathrm{p}}\theta)^{\mathrm{i}} + (\rho L)^{\mathrm{i}}, \tag{3.25}$$

where θ and c_{p} are the potential temperature and the specific heat capacity, respectively, of seawater or sea ice (as indicated), and L is the latent heat of freezing of seawater. The rate of change of the total stored heat is then a heat flux ($\mathrm{W\,m^{-3}}$). While 'stored heat' may be a thermodynamically questionable notion, its rate of change is a well-defined quantity.

In the second term on the LHS of (3.24), $\Sigma\rho\boldsymbol{u}H^{\mathrm{io}}$ is the total ice and ocean sensible and latent heat flux crossing the defined boundary ($\mathrm{W\,m^{-2}}$) and its divergence is the total boundary heat flux ($\mathrm{W\,m^{-3}}$). It has the same form as (3.25) but with each term on the RHS of (3.25) multiplied by either $\boldsymbol{u}^{\mathrm{i}}$ or $\boldsymbol{u}^{\mathrm{o}}$ as appropriate. The sum of the rate of change of stored heat and the divergence of the ice and ocean heat flux ((3.24), LHS) is balanced ((3.24), RHS) by the convergence of heat fluxes by all turbulent and radiative processes at the boundary ($\boldsymbol{F}_{\mathrm{H}}^{\mathrm{bdy}}$; $\mathrm{W\,m^{-2}}$), and the (internal) rate of dissipation of kinetic energy into heat (ϵ; $\mathrm{W\,kg^{-1}}$).

The four terms of (3.24) are next integrated with respect to volume. For scale, the expected total ice and ocean boundary heat flux is expected to be of order 200 TW, and the FW flux 200 mSv (e.g. [9]). First, considering the second term on the RHS of (3.24): with a typical value for $\epsilon \sim 10^{-9}\ \mathrm{W\,kg^{-1}}$ (e.g. [38]), using $\rho = 1000\ \mathrm{kg\,m^{-3}}$, and taking a surface area scale of $10^{13}\ \mathrm{m^2}$ and a depth of 1000 m, we find a total rate of kinetic energy dissipation *ca* 10^{10} W (0.01 TW), which is, as usual, negligible. Second, the first term on the LHS becomes a heat flux (W) equal to the rate of change of the total heat stored within the defined boundary, whether as latent heat (ice) or as sensible heat (ice and ocean). This term is denoted $F_{\mathrm{H}}^{\mathrm{stor}}$ below.

Third, the first term on the RHS, after integration with respect to volume and application of Gauss's theorem, and noting the sign convention for $\boldsymbol{n}$:

$$\iint \boldsymbol{F}_{\mathrm{H}}^{\mathrm{bdy}}\cdot\boldsymbol{n}\,\mathrm{d}s\,\mathrm{d}z = -\left(F_{\mathrm{H}}^{\mathrm{surf}} + F_{\mathrm{H}}^{\mathrm{bed}}\right). \tag{3.26}$$

The scalars on the RHS represent ($F_{\mathrm{H}}^{\mathrm{surf}}$) the total surface flux of heat, which is in turn the sum of radiative (long-wave and short-wave) and turbulent (sensible and latent) heat fluxes, and

($F_{\mathrm{H}}^{\mathrm{bed}}$) the geothermal heat flux at the sea bed. Geothermal heating is also small: at approximately 50 mW m^{-2} (e.g. [39]) and using a scale area 10^{13} m^2, it yields 0.5 TW, again negligible.

Fourth, the second term on the LHS of (3.24), after integration with respect to volume and application of Gauss's theorem, decomposes thus:

$$\iint \Sigma \rho H^{\mathrm{io}} \boldsymbol{u} \cdot \boldsymbol{n} \, \mathrm{d}s \, \mathrm{d}z = -\iint [(v\rho c_{\mathrm{p}}\theta)^{\mathrm{o}} + (v\rho c_{\mathrm{p}}\theta)^{\mathrm{i}} + (v\rho L)^{\mathrm{i}}] \, \mathrm{d}s \, \mathrm{d}z, \tag{3.27}$$

where, on the RHS of (3.27), the three components represent the ocean and ice sensible, and the ice latent, heat fluxes, respectively. While the latent heat flux is an unambiguous (absolute) quantity, the sensible heat flux is not. However, its ambiguity can be quantified by decomposing θ and v into the sums of their means and their anomalies from the mean (cf. equations (3.16) and (3.17)). Taking $\rho = 1000\,\mathrm{kg\,m^{-3}}$, $c_{\mathrm{p}} = 4000\,\mathrm{J\,kg^{-1}\,{}^{\circ}C^{-1}}$, the product $\bar{v}A = 0.2 \times 10^6\,\mathrm{m^3\,s^{-1}}$ and $\bar{\theta} = 1^{\circ}$C [9] yields a 'flux of the mean' of $\rho c_{\mathrm{p}} \bar{\theta} \bar{v} A = 0.8$ TW. This is also negligible. Should it be desired, this flux of the mean can be eliminated by use of a reference temperature of $\bar{\theta}$.

A further term which could be included in the RHS of (3.27) is the heat flux due to rivers, which deliver warm water to the ocean during the few months of the summer melt season. For a scale estimate, we assume a temperature difference (above the mean) of 5°C [40], ρ and c_{p} as before, and a volume flux over the melt season of $10^5\,\mathrm{m^3\,s^{-1}}$ [41]. This equals approximately 2 TW over the melt season for the whole Arctic Ocean, or less than 1 TW over the full calendar year. This may have important impacts local to the environs of river discharges but is small in a pan-Arctic sense.

A final source of uncertainty is the extent to which potential temperature is not a conservative variable [36]. This is related to variation with temperature and salinity of c_{p}, as discussed by Bacon & Fofonoff [34]. For temperatures of $0 \pm 2^{\circ}$C and for salinities of 35 ± 2, this uncertainty is approximately equivalent to a temperature uncertainty of 0.1°C [36, fig. 2]. Taking values of ρ and c_{p} as before and assuming a volume flux of $10^6\,\mathrm{m^3\,s^{-1}}$ (1 Sv), a heat flux uncertainty of 0.4 TW results. This source of uncertainty has greater potential significance in much warmer (tropical) regions of the planet.

Finally, therefore, equation (3.28) expresses the balance between surface and boundary heat fluxes and heat storage, to an accuracy of *ca* 1%:

$$F_{\mathrm{H}}^{\mathrm{surf}} = -\iint [(v'\rho c_{\mathrm{p}}\theta')^{\mathrm{o}} + (v'\rho c_{\mathrm{p}}\theta')^{\mathrm{i}} + (v\rho L)^{\mathrm{i}}] \, \mathrm{d}s \, \mathrm{d}z + F_{\mathrm{H}}^{\mathrm{stor}}, \tag{3.28}$$

and where anomalies of v and θ about their means are introduced following the discussion after (3.27). The integral on the RHS of (3.28) is labelled $F_{\mathrm{H}}^{\mathrm{io}}$ in figure 4. A small error is introduced by use of θ' in (3.28), because of the difference in size of the product (ρc_{p}) between ice and ocean. For scale, we take $c_{\mathrm{p}}^{\mathrm{i}} = 3000$ and $c_{\mathrm{p}}^{\mathrm{o}} = 4000\,\mathrm{J\,kg^{-1}\,{}^{\circ}C^{-1}}$, $\rho^{\mathrm{i}} = 900$ and $\rho^{\mathrm{o}} = 1000\,\mathrm{kg\,m^{-3}}$, $\theta' = 1^{\circ}$C, $v' = 0.1\,\mathrm{m\,s^{-1}}$, width of sea ice of 100 km and thickness 1 m. The resulting error in heat flux is approximately 0.01 TW (per °C), and is negligible, therefore.

Considering the stationary state in (3.28) where $F_{\mathrm{H}}^{\mathrm{stor}} = 0$, and ignoring sea ice to simplify: warm water enters the Arctic (θ' and v' positive), and cooled water leaves (θ', v' negative). The term $(v'\rho c_{\mathrm{p}}\theta')^{\mathrm{o}}$ is positive, the RHS of (3.28) is negative, and so, therefore, is the surface heat flux ((28), LHS), representing loss of heat. This demonstrates the reason for removing the flux of the mean: should water enter and leave the defined volume with no change of temperature (or phase), there is no heat flux.

4. Results

In this section, we present illustrations of the calculation of fluxes and storage of volume, heat and FW using NEMO model output (§2). Figure 1 shows the seasonal cycle of $F_{\mathrm{vol}}^{\mathrm{surf}}$ and $F_{\mathrm{vol}}^{\mathrm{io}}$ and their sum, $\dot{V}$ (3.23). Figure 2 shows the first and third terms from the RHS of (3.22), the boundary integral and salinity storage terms. Figure 3 shows the seasonal cycles of the three components of

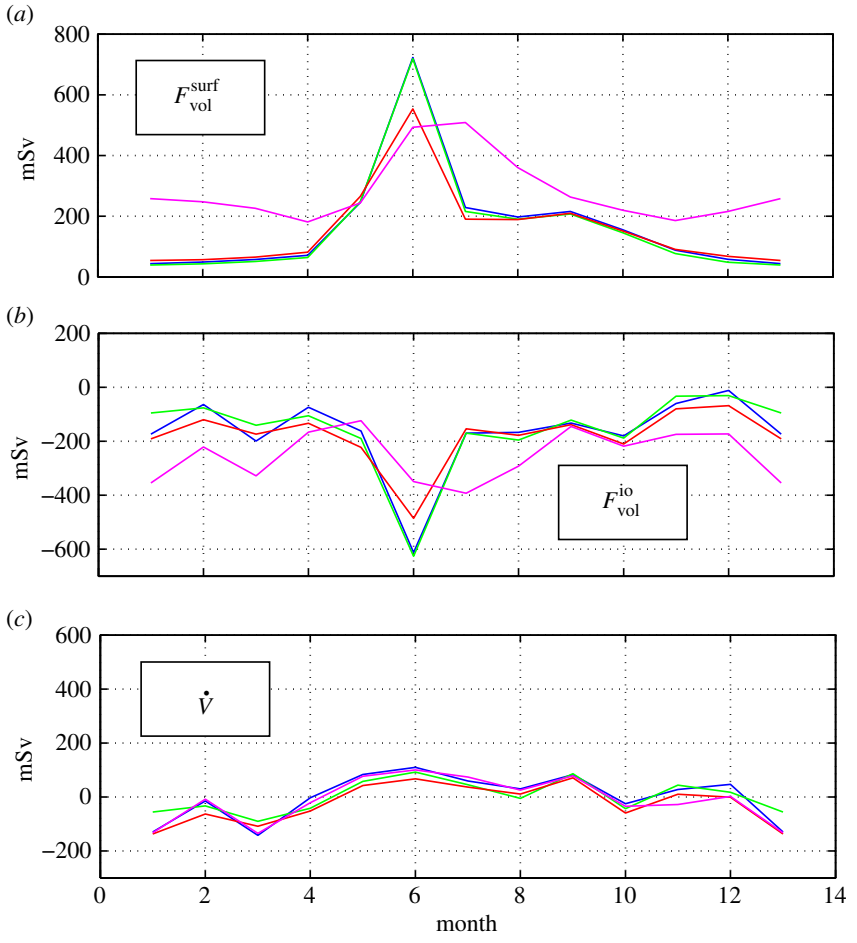

Figure 1. (*a*) Surface volume flux; (*b*) boundary volume flux; and (*c*) total of surface and boundary volume flux (the storage flux). Colours indicate model runs, where purple is 1/12° model; others are 1/4° runs, where red is ERA-Interim, blue is long CORE-II and green is short CORE-II. Month 13 is a repeat of month 1.

the boundary heat flux: sea ice latent, sea ice sensible and ocean (liquid) sensible; figure 4 shows the total surface heat flux, the sum of the three components of the boundary heat flux, and the sum of surface and boundary fluxes (i.e. storage) (3.24).

We consider volume fluxes first. The surface inputs all show similar behaviour, with a summer spike in the net input, which is dominated by the consequences of the seasonal thaw, particularly river flows. The ocean boundary transports are almost a reflection of the surface inputs, which is a consequence of the use of monthly (rather than shorter-time-scale) averages. The sum of surface and boundary flows is storage, which totals 0 ± 78 mSv (1/12°) and $(6–15) \pm (60–80)$ mSv (1/4°) over the year. While the surface and boundary components are different between model realizations, there is a remarkable similarity across the four storage cycles. There is a consistent tendency to accumulate mass within the boundary over summer and to release the stored mass in winter. We hypothesize that this is a consequence of the modulation of (seasonally varying) wind stress curl and consequent changes in Ekman pumping by (seasonal) changes in sea ice properties (including extent, thickness, concentration and strength); cf. Giles *et al.* [42] and Tsamados *et al.* [43]. Testing of this hypothesis is beyond the scope of the present paper, and other processes may be involved. There is a practical conclusion: FW fluxes derived from marine measurements made between August and December should be unbiased with respect to mass storage.

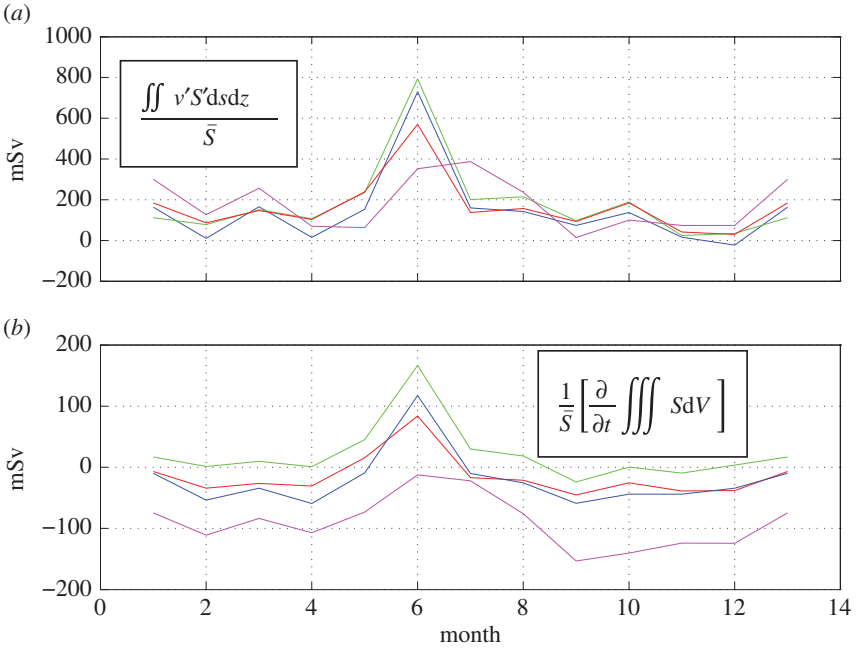

Figure 2. (*a*) Boundary FW flux and (*b*) FW dilution flux. Colours as in figure 1.

The volume flux calculation provides two of the four elements of (3.22): $F_{\mathrm{vol}}^{\mathrm{surf}}$ and $\dot{V}$. The other two terms are $\iiint v'S'\,\mathrm{d}s\,\mathrm{d}z/\bar{S}$ (the FW boundary flux) and $(1/\bar{S})(\partial(\iiint S\,\mathrm{d}V)/\partial t)$ the dilution flux. It is clear that, outside the months of summer melt, modelled variability in both the FW boundary flux and the dilution flux is low, but both terms show a significant peak within the melt months. Ice and ocean measurements need to include the melt period if estimates of annual mean FW fluxes are to be unbiased.

We finally consider heat fluxes. We note that the sea ice sensible heat flux is small—about 1% of the total—so in practice it can usually be neglected, and another small term is the heat input due to rivers. The liquid sensible heat flux is, then, the largest component of the total, with a clear seasonal cycle: a late-winter (May) minimum of 50–100 TW (approx. 3–7 W m^{-2}) and an autumn (October) maximum of 150–200 TW (approx. 11–14 W m^{-2}). The sea ice latent heat transport is an important contributor to the total, with a clear and somewhat asymmetric seasonal cycle: the summer (August) minimum is 5–10 TW, the winter (March) maximum is 50–80 TW. The sum of all three components retains a seasonal cycle; there is an indication that the $1/12^{\circ}$ model boundary heat fluxes are high relative to the $1/4^{\circ}$ fluxes, which may be a consequence of better resolution of ocean inflows and outflows to/from the defined volume. As a practical consideration, it may be that measured estimates of ice and ocean heat fluxes made in autumn are biased high with respect to the annual mean. The relatively 'flat' boundary heat flux seasonal cycle, *ca* 150 ± 50 TW (approx. 11 ± 3 W m^{-2}), is contrasted to the (relatively) very large seasonal cycle in surface fluxes, with a range approximately ± 500 TW (30 W m^{-2}), which, as a consequence, dominates the sum of surface and boundary fluxes (storage). This implies that a large fraction of the cycle whereby heat is absorbed and released by ice and ocean within the defined volume is local and intra-annual. We note that surface heat fluxes are regionally dominated by the open waters of the Barents Sea, at 60–70% of the total (not shown).

5. Discussion

The aim of this paper was to present a method for calculating ice and ocean fluxes of mass, heat and FW. The method includes advances over previous publications through explicit consideration

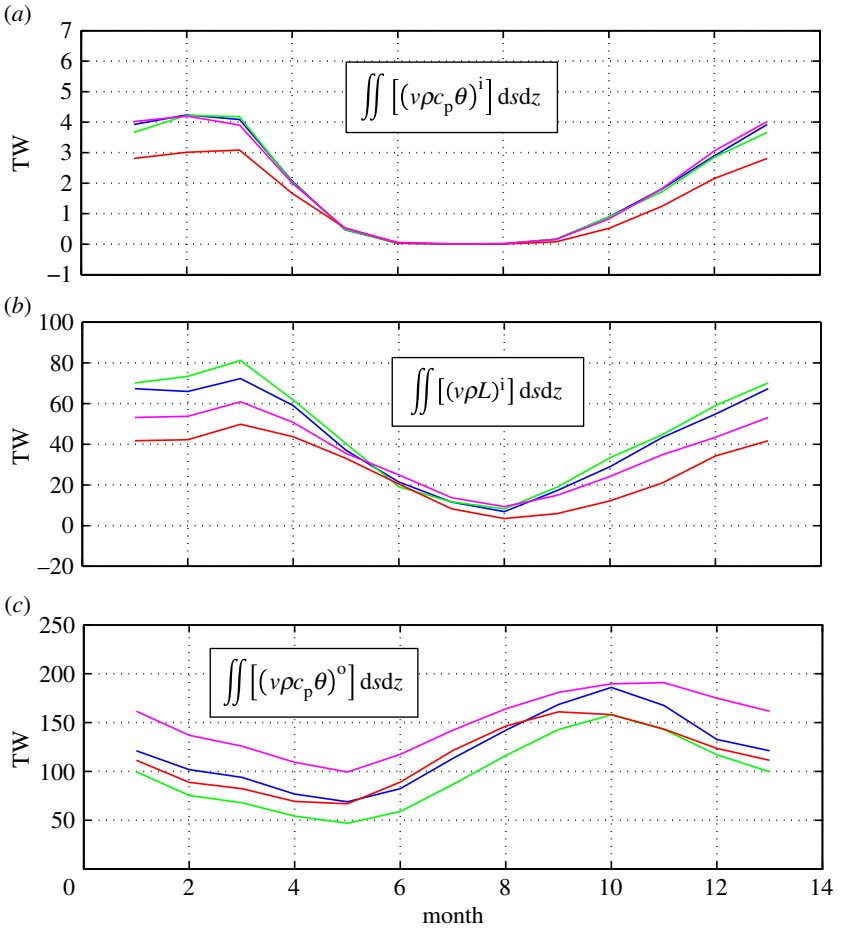

Figure 3. (*a*) Ice sensible boundary heat flux; (*b*) ice latent boundary heat flux; and (*c*) liquid sensible boundary heat flux. Colours as in figure 1.

of temporal variability and storage. Arbitrary 'reference values' are eliminated from FW fluxes and their role clarified for heat fluxes. We illustrated the application of the method using model output, and note that the results are tolerably robust (i.e. similar in magnitude and phase) across the range of available model configurations. We note next the viability of this new approach using available *in situ* and remote-sensed measurements. The seminal paper on Arctic FW fluxes is by Aagaard & Carmack [44], in which the authors estimated the surface flux of FW in two ways, which they called 'direct' and 'indirect'. The direct method entailed estimating the contributions of evaporation, precipitation and run-off to the total. This is the calculation of $F_{\mathrm{vol}}^{\mathrm{surf}}$, in our terms, and it remains problematic in practice today, through issues such as ungauged run-off and weaknesses in reanalysis products. The indirect method employed ice and ocean measurements to the same end, and this is analogous to our FW boundary flux. Tsubouchi *et al.* [9] have demonstrated the practicability of making (quasi-) synoptic boundary flux estimates, so that the first term on the RHS of (3.22) is accessible from ice and ocean measurements, in principle. Gravity (mass) measurements from satellites show that the mass storage term (the second term on the RHS of (3.22)) can be measured for the Arctic [45]. For the dilution flux (the third term on the RHS of (3.22)), two independent methods have been used to estimate this term in the Arctic: an *in situ* salinity census [46], and a combination of satellite gravity and altimetric sea surface height measurements [42]. Therefore—in principle—it is practicable to generate complete estimates, on

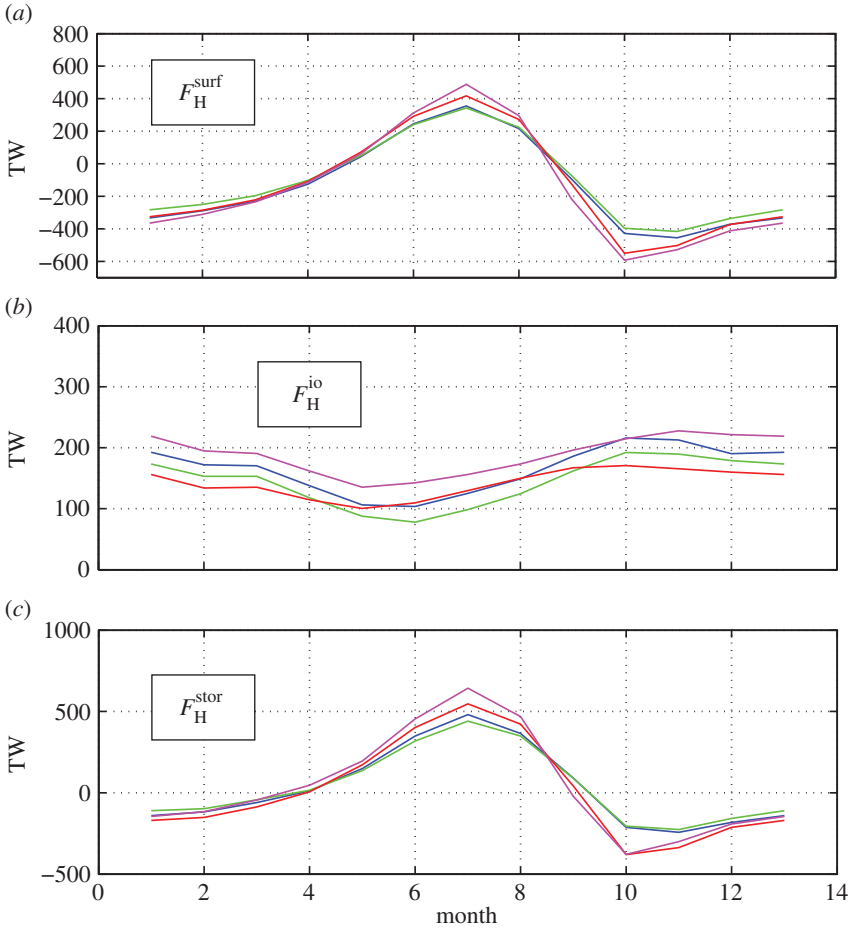

Figure 4. (*a*) Total surface heat flux; (*b*) total boundary heat flux; and (*c*) total of surface and boundary heat flux (storage). Colours as in figure 1.

a monthly time scale, of mass and FW fluxes and storage. Heat fluxes and storage should be similarly accessible to measurement.

We wish to explore the meaning of the idea of a 'FW flux'. Many authors expend more effort in deciding on a 'correct' reference value for ocean FW calculations than on considering the meaning of the calculation. We attempt to clarify. How is it possible to calculate (in this case) an Arctic surface FW flux from ice and ocean measurements when the flux is so small (of order 200 mSv) in comparison to the seawater transports from which they are derived (of order 10 Sv), and given the accuracy with which such transports can be measured? The latter is approximately 10% for instruments capable of absolute accuracy of current speed measurement of order a few centimetres per second—therefore approximately 1 Sv, an order of magnitude greater than the FW signal. Consider an approximate version of (3.22) wherein we assume stationarity and so ignore storage. We express the surface flux in terms of a mean, net, ice and ocean inflow (V_O), balanced by a similar outflow, modified by a surface FW flux, thus

$$F_{vol}^{surf} \approx \left(\frac{\delta S}{\bar{S}}\right) V_O, \tag{5.1}$$

where δS is now the salinity difference between inflow and outflow. The calculation has skill as a result of the high accuracy with which we can measure salinity (assuming adequate spatial

resolution). The dominant *relative* uncertainty is still that of the measurements comprising V_O, but it is now scaled by the term in parentheses. The RHS expresses, therefore, the scaled change of inflow salinity into outflow salinity (by dilution, in this case) caused by F^{surf}.

The meaning of a surface flux of FW is clear and unambiguous. The meaning of an 'ocean FW flux' is clarified by consideration of (5.1). There must exist, at least implicity, a closed volume whose upper surface supplies the FW flux that modifies salinity from inflow to outflow. Then a value of boundary-mean salinity can be calculated (i.e. $\bar{S}$)—this is the only correct number to employ in the role of 'reference value'. Then, further, there is a physical, non-arbitrary meaning to 'ocean FW flux': it is the FW that must have been added (or removed) to dilute (or concentrate) inflow to outflow salinity. This has uncomfortable consequences. In principle, 'reference values' can change: according to the geographical location of the (actual or assumed) boundary, and from month to month, or year to year, although as noted by Tsubouchi *et al*. [9], in practice and for the present, defined, pan-Arctic boundary, the seasonal change is small—their PHC-derived estimates of mean salinity (including sea ice) are 34.68 (winter) and 34.69 (summer). Furthermore, there is no special role in this context for the interior (volume) mean property value.

In practice, where the product of anomalies is specified—as in (3.22)—only one of the two quantities need to be a properly constructed (i.e. zero mean) anomaly. Integration of the product of an anomaly term with an arbitrarily referenced second term formally eliminates any non-zero mean. If an arbitrary salinity reference is used, then the extent to which the calculation is in error depends on context, and we provide three illustrations.

Following the derivation of the calculation of F^{surf} from §3.2, but now using a reference salinity (S_{ref}) and the anomaly about the reference value ($S^\dagger$):

$$S = \bar{S} + S' = S_{\text{ref}} + S^\dagger. \tag{5.2}$$

We expand the integral of (3.18) with this expression of salinity, and neglect ρ for simplicity:

$$\iint [\bar{v} + v'][S_{\text{ref}} + S^\dagger]\,\mathrm{d}s\,\mathrm{d}z = S_{\text{ref}}\bar{v}\iint \mathrm{d}s\,\mathrm{d}z + \bar{v}\iint S^\dagger\,\mathrm{d}s\,\mathrm{d}z + S_{\text{ref}}\iint v'\,\mathrm{d}s\,\mathrm{d}z + \iint v'S^\dagger\,\mathrm{d}s\,\mathrm{d}z. \tag{5.3}$$

We consider each term on the RHS in order. For the first term:

$$S_{\text{ref}}\bar{v}\iint \mathrm{d}s\,\mathrm{d}z = S_{\text{ref}}F^{\text{io}}_{\text{vol}}. \tag{5.4}$$

For the second term, and noting that anomalies from the mean integrate to zero:

$$\bar{v}\iint S^\dagger\,\mathrm{d}s\,\mathrm{d}z = \bar{v}\iint (\bar{S} + S' - S_{\text{ref}})\,\mathrm{d}s\,\mathrm{d}z = (\bar{S} - S_{\text{ref}})F^{\text{io}}_{\text{vol}}. \tag{5.5}$$

The third term integrates to zero. The fourth term is

$$\iint v'S^\dagger\,\mathrm{d}s\,\mathrm{d}z = \iint v'(\bar{S} + S' - S_{\text{ref}})\,\mathrm{d}s\,\mathrm{d}z = \iint v'S'\,\mathrm{d}s\,\mathrm{d}z. \tag{5.6}$$

Summation of the four terms eliminates the pair of $S_{\text{ref}}F^{\text{io}}_{\text{vol}}$ terms, and therefore returns the same as the RHS of (3.18), in 'volume' form. However, there are two assumptions here: (i) that the calculation is correctly posed from the start and (ii) that the integral follows the complete circuit of the boundary. We next consider the impact of each of these assumptions in turn.

Key to the method is the definition of the boundary-mean values of salinity and velocity, their anomalies about their means and the emergence of the boundary-mean salinity as a 'natural' analogue to a reference value. Thus, in (3.21) and (3.22), $\bar{S}$ appears on the denominator and S' appears under the integral in the numerator. We next examine the consequence of assuming a 'traditional' form for the calculation of FW fluxes, which we denote $F^\dagger$, and expand, still assuming that the integral follows the complete circuit of the boundary:

$$F^\dagger = \frac{\iint v'S^\dagger\,\mathrm{d}s\,\mathrm{d}z}{S_{\text{ref}}} = \frac{\iint v'(\bar{S} + S' - S_{\text{ref}})\,\mathrm{d}s\,\mathrm{d}z}{S_{\text{ref}}} = \frac{\iint v'S'\,\mathrm{d}s\,\mathrm{d}z}{S_{\text{ref}}}. \tag{5.7}$$

Thus $F^{\dagger}$ is only in error in comparison to the first terms of the RHS of (3.21) and (3.22) by a factor $(\bar{S}/S_{\mathrm{ref}})$, which is very small. If $S_{\mathrm{ref}} = 34.9$ and $\bar{S} = 34.7$, then the error is 0.6%.

Finally, we consider the error introduced by the use of the 'traditional' form $F^{\dagger}$ but where the integral does not follow the complete circuit of the boundary. Rather, it is only applied to a component, such as a single strait or current. For this partial circuit, the velocity anomaly no longer integrates to zero, so that (5.7) must be considered in the intermediate form:

$$F^{\dagger} = \frac{\iint v'(\bar{S} + S' - S_{\mathrm{ref}})\,\mathrm{d}s\,\mathrm{d}z}{S_{\mathrm{ref}}} = \frac{\delta S \iint v'\,\mathrm{d}s\,\mathrm{d}z}{S_{\mathrm{ref}}} + \frac{\iint v'S'\,\mathrm{d}s\,\mathrm{d}z}{S_{\mathrm{ref}}}, \tag{5.8}$$

where $\delta S = \bar{S} - S_{\mathrm{ref}}$ is the difference between the boundary-mean salinity and the assumed reference salinity. The second term on the RHS of (5.8) is the true FW flux component through the chosen strait, or across the chosen current, but scaled by the factor $(\bar{S}/S_{\mathrm{ref}})$, so it is only slightly in error. However, the first term on the RHS of (5.8) is potentially an important source of error, because the term $\iint v'\,\mathrm{d}s\,\mathrm{d}z$ is (very nearly) the seawater volume transport across the current or strait, and it is multiplied by the ratio $(\delta S/S_{\mathrm{ref}})$. If $\delta S = 0.2$ and $S_{\mathrm{ref}} = 34.9$, then the ratio equals 6×10^{-3}. This translates to a FW transport error of 6 mSv per Sv of seawater transport. For the East Greenland Current in Fram Strait with a seawater transport of approximately 5 Sv, for example, a reference value in error by 0.2 in salinity would generate a FW flux error of order 30 mSv.

As a concluding point of interest, we observe that the complete boundary integral can be split into its component currents or straits, and we illustrate this procedure with the stationary case applied to the same boundary defined in §2:

$$F^{\mathrm{surf}}_{\mathrm{vol}} = \frac{\iint v'S'\,\mathrm{d}s\,\mathrm{d}z}{\bar{S}} = F^{\mathrm{io}}_{\mathrm{Ber}} + F^{\mathrm{io}}_{\mathrm{Dav}} + F^{\mathrm{io}}_{\mathrm{BSO}} + F^{\mathrm{io}}_{\mathrm{FSW}} + F^{\mathrm{io}}_{\mathrm{FSE}}, \tag{5.9}$$

where the abbreviations refer to Bering Strait (*Ber*), Davis Strait (*Dav*), the Barents Sea Opening (*BSO*), Fram Strait West (*FSW*, including the East Greenland Current), and Fram Strait East (*FSE*, including the West Spitzbergen Current). Our approach starts from the net surface flux of FW, and (broadly) we interpret this approach to mean the quantification of the dilution of (mainly) saline inflows to the Arctic Ocean into freshened outflows. This approach is elucidated in Tsubouchi *et al.* [9]. However, analysts of Arctic FW budgets often like to consider the Bering Strait to be a source of FW to the Arctic Ocean (e.g. [47]), and the decomposition of (5.9) clarifies the meaning of this hybrid approach. Inflows to the Arctic have v' signed positive (and vice versa), and saline waters have S' signed positive (and vice versa) similarly. At the most simple level, the inflows among the straits and currents in (5.9) are Bering Strait (−), Fram Strait East (+) and the BSO (+); Davis Strait (−) and Fram Strait West (−) are outflows; and the signs in parentheses indicate whether they are fresher or more saline than the boundary mean. Taking the products of the signs of the velocity and salinity anomalies outside the magnitude of the component FW fluxes, we have

$$F^{\mathrm{surf}}_{\mathrm{vol}} = \frac{\iint v'S'\,\mathrm{d}s\,\mathrm{d}z}{\bar{S}} = -\left|F^{\mathrm{io}}_{\mathrm{Ber}}\right| + \left|F^{\mathrm{io}}_{\mathrm{Dav}}\right| + \left|F^{\mathrm{io}}_{\mathrm{BSO}}\right| + \left|F^{\mathrm{io}}_{\mathrm{FSW}}\right| + \left|F^{\mathrm{io}}_{\mathrm{FSE}}\right|. \tag{5.10}$$

It is seen from (5.10) that moving $F^{\mathrm{io}}_{\mathrm{Ber}}$ from the RHS to the LHS makes this statement: that the addition of the surface FW flux to the relatively fresh Bering Strait ocean inflow to the Arctic acts to dilute the Atlantic inflows (the West Spitsbergen Current in Fram Strait East, and the BSO) into the freshened outflows of Davis Strait and (in Fram Strait West) the East Greenland Current.

Competing interests. We declare we have no competing interests.

Funding. This work was partly funded by, and is a contribution to, the UK Natural Environment Research Council's TEA-COSI project, as part of its Arctic Research Programme.

Acknowledgements. The authors are grateful to the referees who provided insightful and helpful comments.

References

1. IPCC. 2013 Climate change 2013: the physical science basis. In *Contribution of Working Group I to the Fifth Assessment Report of the Intergovernmental Panel on Climate Change* (eds TF Stocker *et al.*). Cambridge, UK: Cambridge University Press.
2. Serreze MC, Barrett AP, Stroeve JC, Kindig DN, Holland MM. 2009 The emergence of surface-based Arctic amplification. *Cryosphere* **3**, 11–19. (doi:10.5194/tc-3-11-2009)
3. Manabe S, Stouffer R. 1995 Simulation of abrupt climate change induced by freshwater input to the North Atlantic Ocean. *Nature* **378**, 165–167. (doi:10.1038/378165a0)
4. Francis JA, Vavrus SJ. 2012 Evidence linking Arctic amplification to extreme weather in mid-latitudes. *Geophys. Res. Lett.* **39**, L06801. (doi:10.1029/2012GL051000)
5. Liu J, Curry JA, Wang H, Song M, Horton RM. 2012 Impact of declining Arctic sea ice on winter snowfall. *Proc. Natl Acad. Sci. USA* **109**, 4074–4079. (doi:10.1073/pnas.1114910109)
6. Petoukhov V, Rahmstorf S, Petri S, Schellnhuber HJ. 2013 Quasiresonant amplification of planetary waves and recent Northern Hemisphere weather extremes. *Proc. Natl Acad. Sci. USA* **110**, 5336–5341. (doi:10.1073/pnas.1222000110)
7. Screen JA, Simmonds I. 2014 Amplified mid-latitude planetary waves favour particular regional weather extremes. *Nat. Clim. Change* **4**, 704–709. (doi:10.1038/NCLIMATE2271)
8. Cowtan K, Way RG. 2014 Coverage bias in the HADCRUT4 temperature series and its impact on recent temperature trends. *Q. J. R. Meteorol. Soc.* **140**, 1935–1944. (doi:10.1002/qj.2297)
9. Tsubouchi T *et al*. 2012 The Arctic Ocean in summer: a quasi-synoptic inverse estimate of boundary fluxes and water mass transformation. *J. Geophys. Res.* **117**, C01024. (doi:10.1029/2011JC007174)
10. Torres-Valdes S *et al*. 2013 Export of nutrients from the Arctic Ocean. *J. Geophys. Res.* **118**, 1625–1644.(doi:10.1002/jgrc.20063)
11. MacGilchrist GA, Naveira Garabato AC, Tsubouchi T, Bacon S, Torres-Valdes S, Azetsu-Scott K. 2014 The Arctic Ocean carbon sink. *Deep-Sea Res. I* **86**, 39–55. (doi:10.1016/j.dsr.2014.01.002)
12. Jahn A *et al*. 2012 Arctic Ocean freshwater: how robust are model simulations? *J. Geophys. Res.* **117**, C00D16. (doi:10.1029/2012JC007907)
13. Lique C, Steele M. 2012 Where can we find a seasonal cycle of the Atlantic water temperature within the Arctic Basin? *J. Geophys. Res.* **117**, C03026. (doi:10.1029/2011JC007612)
14. Bacon S, Marshall A, Holliday NP, Aksenov Y, Dye S. 2014 Seasonal variability of the East Greenland Coastal current. *J. Geophys. Res.* **119**, 3967–3987. (doi:10.1002/2013JC009279)
15. Madec G, NEMO team. 2011 *NEMO Ocean Engine, version 3.3, Note du Pole de Modelisation*. Paris, France: Institut Pierre-Simon Laplace.
16. Fichefet T, Morales Maqueda M. 1997 Sensitivity of a global sea ice model to the treatment of ice thermodynamics and dynamics. *J. Geophys. Res.* **102**, 12 609–12 646. (doi:10.1029/97JC00480)
17. Smith W, Sandwell D. 1997 Global sea floor topography from satellite altimetry and ship depth soundings. *Science* **277**, 1956–1962. (doi:10.1126/science.277.5334.1956)
18. Jakobsson M, Macnab R, Mayer L, Anderson R, Edwards M, Hatzky J, Schenke HW, Johnson P. 2008 An improved bathymetric portrayal of the Arctic Ocean: implications for ocean modeling and geological, geophysical and oceanographic analyses. *Geophys. Res. Lett.* **35**, L07602. (doi:10.1029/2008GL033520)
19. Jackett DR, McDougall TJ. 1995 Minimal adjustment of hydrographic data to achieve static stability. *J. Atmos. Oceanic Technol.* **12**, 381–389. (doi:10.1175/1520-0426(1995)012<0381:MAOHPT>2.0.CO;2)
20. Levitus S, Boyer T, Conkright M, O' Brien T, Antonov J, Stephens C, Stathoplos L, Johnson D, Gelfeld R. 1998 *NOAA Atlas NESDIS 18, World Ocean Database 1998, Introduction*, vol. 1. Washington, DC: US Government Printing Office.
21. Levitus S, Boyer T, Conkright M, Johnson D, O' Brien T, Antonov J, Stephens C, Gelfeld R. 1998 *NOAA Atlas NESDIS 19, World Ocean Database 1998, Temporal Distribution of Mechanical Bathythermograph Profiles*, vol. 2. Washington, DC: US Government Printing Office.
22. Steele M, Morley R, Ermold W. 2001 PHC: a global ocean hydrography with a high-quality Arctic Ocean. *J. Clim.* **14**, 2079–2087. (doi:10.1175/1520-0442(2001)014<2079:PAGOHW>2.0.CO;2)
23. Nurser AJG, Bacon S. 2014 The Rossby radius in the Arctic Ocean. *Ocean Sci.* **10**, 967–975. (doi:10.5194/os-10-967-2014)

24. Barnier B *et al*. 2006 Impact of partial steps and momentum advection schemes in a global ocean circulation model at eddy permitting resolution. *Ocean Dyn.* **56**, 543–567. (doi:10.1007/s10236-006-0090-1)
25. Levier B, Treguier A-M, Madec G, Garnier V. 2007 Free surface and variable volume in the NEMO code. MERSEA IP Rep. WP09-CNRS-STR-03–1A, IFREMER, Brest, France.
26. Brodeau L, Barnier B, Treguier A-M, Penduff T, Gulev S. 2010 An ERA40-based atmospheric forcing for global ocean circulation models. *Ocean Model.* **31**, 88–104. (doi:10.1016/j.ocemod.2009.10.005)
27. Large WG, Yeager SG. 2009 The global climatology of an interannually varying air–sea flux data set. *Clim. Dyn.* **33**, 341–364. (doi:10.1007/s00382-008-0441-3)
28. Dee DP *et al*. 2011 The ERA-Interim reanalysis: configuration and performance of the data assimilation system. *Q. J. R. Meteorol. Soc.* **137**, 553–597. (doi:10.1002/qj.828)
29. Large WG, Yeager SG. 2004 Diurnal to decadal global forcing for ocean and sea-ice models: the data sets and flux climatologies. Technical Note NCAR/TN-460+STR. Boulder, CO: National Center for Atmospheric Research.
30. Gill AE. 1982 *Atmosphere-ocean dynamics*. London, UK: Academic Press.
31. Starr VP. 1951 Applications of energy principles to the general circulation. In *Compendium of meteorology* (ed. TF Malone), pp. 568–574. Boston, MA: American Meteorological Society.
32. Bryan K. 1962 Measurements of meridional heat transport by ocean currents. *J. Geophys. Res.* **67**, 3403–3414. (doi:10.1029/JZ067i009p03403)
33. Saunders PM. 1995 The Bernoulli function and flux of energy in the ocean. *J. Geophys. Res.* **100**, 22 647–22 648. (doi:10.1029/95JC02614)
34. Bacon S, Fofonoff N. 1996 Oceanic heat flux calculation. *J. Atmos. Oceanic Technol.* **13**, 1327–1329. (doi:10.1175/1520-0426(1996)013<1327:OHFC>2.0.CO;2)
35. Warren BA. 1999 Approximating the energy transport across oceanic sections. *J. Geophys. Res.* **104**, 7915–7919. (doi:10.1029/1998JC900089)
36. McDougall TJ. 2003 Potential enthalpy: a conservative oceanic variable for evaluating heat content and heat fluxes. *J. Phys. Oceanogr.* **33**, 945–963. (doi:10.1175/1520-0485(2003)033<0945:PEACOV>2.0.CO;2)
37. Serreze MC, Barrett AP, Slater AG, Steele M, Zhang J, Trenberth KE. 2007 The large-scale energy budget of the Arctic. *J. Geophys. Res.* **112**, D11122. (doi:10.1029/2006JD008230)
38. Rippeth T, Lincoln BJ, Lenn Y-D, Green JAM, Sundfjord A, Bacon S. 2015 Tide-mediated warming of the Arctic halocline by Atlantic water heat fluxes over rough topography. *Nat. Geosci.* **8**, 191–194. (doi:10.1038/NGEO2350)
39. Timmermans M-L, Garrett C. 2006 Evolution of the deep water in the Canadian Basin in the Arctic Ocean. *J. Phys. Oceanogr.* **36**, 866–874. (doi:10.1175/JPO2906.1)
40. Nghiem SV, Hall DK, Rigor IG, Li P, Neumann G. 2014 Effects of Mackenzie River discharge and bathymetry on sea ice in the Beaufort Sea. *Geophys. Res. Lett.* **41**, 873–879. (doi:10.1002/2013GL058956)
41. Fisher JA, Jacob DJ, Soerensen AL, Amos HM, Steffen A, Sunderland EM. 2012 Riverine source of Arctic Ocean mercury inferred from atmospheric observations. *Nat. Geosci.* **5**, 499–504. (doi:10.1038/NGEO1478)
42. Giles KA, Laxon SW, Ridout AL, Wingham DJ, Bacon S. 2012 Western Arctic Ocean freshwater storage increased by wind-driven spin-up of the Beaufort Gyre. *Nat. Geosci.* **5**, 194–197. (doi:10.1038/NGEO1379)
43. Tsamados M, Feltham DL, Schroeder D, Flocco D, Farrell SL, Kurtz NT, Laxon SW, Bacon S. 2014 Impact of variable atmospheric and oceanic form drag on simulations of Arctic sea ice. *J. Phys. Oceanogr.* **44**, 1329–1353. (doi:10.1175/JPO-D-13-0215.1)
44. Aagaard K, Carmack EC. 1989 The role of sea ice and other fresh water in the Arctic circulation. *J. Geophys. Res.* **94**, 14 485–14 498. (doi:10.1029/JC094iC10p14485)
45. Peralta-Ferriz C, Morison J. 2010 Understanding the annual cycle of the Arctic Ocean bottom pressure. *Geophys. Res. Lett.* **37**, L10603. (doi:10.1029/2010GL042827)
46. Rabe B, Karcher M, Kauker F, Schauer U, Toole JM, Krishfield RA, Pisarev S, Kikuchi T, Su J. 2014 Arctic Ocean basin liquid freshwater storage trend 1992–2012. *Geophys. Res. Lett* **41**, 961–968. (doi:10.1002/2013GL058121)
47. Haine TWN *et al*. 2015 Arctic freshwater export: status, mechanisms, and prospects. *Glob. Planet. Change* **125**, 13–35. (doi:10.1016/j.gloplacha.2014.11.013)